



Cite this: DOI: 10.1039/d6cc00319b

 Received 16th January 2026,
Accepted 12th March 2026

DOI: 10.1039/d6cc00319b

rsc.li/chemcomm

A solid-phase click² strategy for chromophore–DNA conjugates and their application as a light harvesting system

 Andreas J. Schmidt,  Annabel M. L. Knispel  and Hans-Achim Wagenknecht *

A stepwise and orthogonal approach of two independent click reactions directly on the solid phase gives easy access to doubly modified DNA. Firstly, 5'-ethynyl-2'-deoxyuridine reacts directly with an azide-modified porphyrin; secondly, 5'-azido-2'-deoxyuridine is generated *in situ* from 5'-iodo-2'-deoxyuridine, which enables a click reaction with an alkyne-functionalized pyrene. The doubly modified DNA was characterized as a light-harvesting system.

Copper-catalyzed azide–alkyne cycloaddition (CuAAC)^{1,2} has emerged as a robust and efficient tool for postsynthetic functionalization of biomolecules, in particular DNA, bypassing the need for complex synthesis of modified phosphoramidites as building blocks for each DNA modification and simplifying the purification of modified DNA.^{3–7} Conventionally, this is achieved using alkyne-bearing building blocks, such as 5'-ethynyl-2'-deoxyuridine (EdU) reacting with organic azides for labelling.⁸ The approach *vice versa* requires the synthesis of a DNA modified with an azide group. However, the inherent instability of many azides during automated DNA synthesis based on phosphorous(III) often restricts this approach and limits it to rare examples in the literature.^{5,9} We solved this issue by synthesizing DNA containing 5-iodo-2'-deoxyuridine (IdU) within the sequence, which can selectively and postsynthetically be modified by ethynyl-modified Nile red as a fluorescent label after *in situ* formation of the intermediate 5-azido-2'-deoxyuridine (AdU).³ Building on this approach, we report herein the combination of EdU and IdU for two independent orthogonal click reactions resulting in a dual click² postsynthetic DNA labelling strategy with full sequence control (Fig. 1).

The desired oligonucleotides **DNA1**, **DNA2** and **DNA3** were designed with a random sequence, the chromophore modifications in the middle and the chromophores in **DNA3** separated by two intervening base pairs, and were synthesized using the readily accessible phosphoramidites of commercially available EdU and IdU for the corresponding precursors **DNA1'**, **DNA2'**

and **DNA3'**. Standard coupling protocols ensured efficient incorporation of both artificial nucleotides into the strand.¹⁰

Afterwards, the presynthesized oligonucleotides (1 μmol) were not cleaved from the solid support (controlled pore glass, CPG). The first postsynthetic modification was achieved by reacting the ethynyl group of EdU as part of the sequence of **DNA1'** and **DNA3'** with the porphyrin azide **1** (10 equiv.) by means of CuAAC (50 equiv. sodium ascorbate, 11 equiv. TBTA ligand,¹¹ 30 equiv. Cu(CH₃CN)₄PF₆, 15 h at room temperature). As anticipated and determined by HPLC, the first click modification proceeded with near-quantitative efficiency. To introduce 1-ethynylpyrene **2** as the first or second label, the azide group of AdU was generated *in situ* from the IdU precursor as part of the presynthesized **DNA2'** or **DNA3'** by treatment with sodium azide (200 μmol in DMSO, 1 h at 50 °C). The resulting oligonucleotide was immediately reacted with 1-ethynylpyrene **2** (50 equiv.) in a click reaction using the same conditions as for the formation of **DNA1**. The selection of pyrene for the second chromophore modification is strategically significant. (i) Its UV/Vis absorption occurs well separated from the porphyrin.

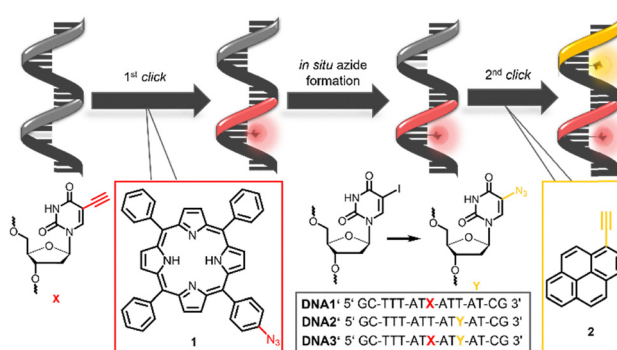


Fig. 1 Dual labelling strategy of presynthesized **DNA3'** by using 5-ethynyl-2'-deoxyuridine (**X**) for the first click reaction with azide **1** and 5-iodo-2'-deoxyuridine converted *in situ* to 5-azido-2'-deoxyuridine (**Y**) for second click modification with alkyne **2**. Presynthesized **DNA1'** and **DNA2'** are controls for single modifications, either with azide **1** (**DNA1**) or with alkyne **2** (**DNA2**).



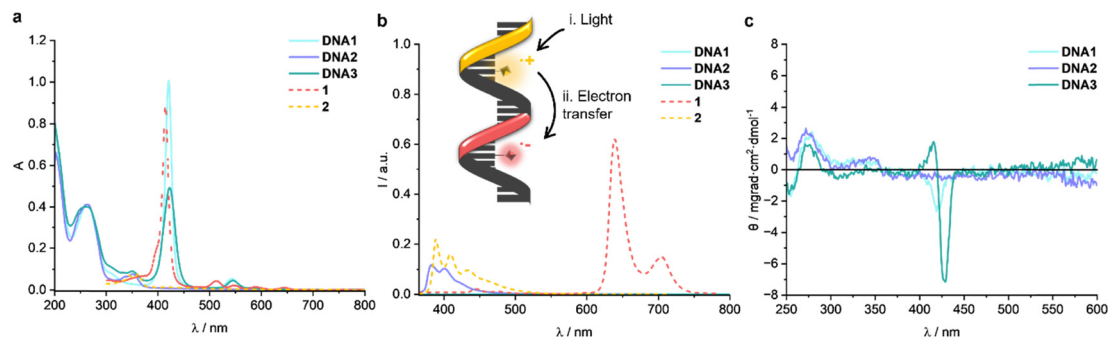


Fig. 2 (a) UV/VIS absorption spectra, (b) fluorescence spectra and (c) circular dichroism spectra of **DNA1–DNA3** (each 2.5 μM in 10 mM sodium phosphate buffer, pH 7.0, 250 mM NaCl) and the unbound chromophores **1** and **2** (each 2.5 μM in DMSO), $\lambda_{\text{exc}} = 350$ nm. The UV/Vis absorption of **1** and **2** was cut off below $\lambda = 300$ nm due to the cut-off effect of DMSO as a solvent.

(ii) 1-Ethynylpyrene is commercially available. (iii) Pyrenes are able to induce an electron transfer in DNA.^{12,13} In conclusion, the pyrene/porphyrin pair is well suited for light-harvesting systems by spectroscopic means.^{14,15} Successful modification to **DNA1–DNA3** was evidenced by ESI mass spectrometry. Interestingly, MS analysis of **DNA1** and **DNA3** showed the coordination of Cu(II), presumably by the presence of the porphyrin as a ligand.

Following successful synthesis of the chromophore–DNA conjugates **DNA1**, **DNA2** and **DNA3**, their photophysical properties were characterized using methods of optical spectroscopy, including UV/vis absorption spectroscopy, steady-state and time-resolved fluorescence spectroscopy, and circular dichroism (CD) spectroscopy (Fig. 2). In the case of pyrene, we could determine a melting temperature of 40 °C for double-stranded **DNA2**. However, the bulky porphyrin modification strongly interferes with annealing and no stable hybridization was observed with complementary unmodified counterstrands to **DNA1** and **DNA3**, and consequently the melting temperatures could not be determined. Consequently, we used only the single strands **DNA1**, **DNA2** and **DNA3** for characterization. Their UV/Vis absorption spectra (Fig. 2a) display the characteristic nucleic acid maximum at $\lambda = 260$ nm together with the pyrene band at $\lambda = 350$ nm and an intense porphyrin Soret band at $\lambda = 419$ nm, accompanied by Q-bands in the range of $\lambda = 550$ – 600 nm.^{16,17} The single strands show also the DNA-characteristic helicity as the circular dichroism (Fig. 2c) reveals the characteristic Cotton effect of B-DNA with a positive band at $\lambda = 275$ nm and a negative band at $\lambda = 250$ nm. A negative Cotton effect within the Soret band characterizes the spatial orientation of the porphyrin macrocycle when intercalated between nucleobase pairs. Significant exciton splitting in the range of $\lambda = 400$ – 450 nm was detected, due to strong ground-state interactions between the two different chromophores in **DNA3**.^{18–20} Minor intensity changes in the base regions merely indicate local structural adjustments in the immediate vicinity of the modification sites.¹⁷ Obviously, two intervening base pairs between the chromophores are sufficient. Compared to chromophores **1** and **2**, the fluorescence spectra (Fig. 2b) show pronounced emission quenching due to covalent binding of these chromophores to **DNA1** and **DNA2**. A significant attenuation of porphyrin fluorescence occurs in the singly labelled **DNA2**. In the doubly labelled **DNA3**, both the porphyrin and pyrene emission are almost completely quenched.

This indicates highly efficient non-radiative decay pathways of the excited state of the chromophores. Time-resolved fluorescence measurements by TCSPC corroborate this interpretation, revealing a drastically shortened average lifetime of $\tau = 0.13$ ns for the emission of **DNA3** at $\lambda_{\text{em}} = 400$ nm when excited at $\lambda_{\text{exc}} = 370$ nm (ns-pulsed LED) compared to typical lifetimes of the unbound pyrene derivative **2** with $\tau_0 = 6.4$ ns, respectively, measured at identical concentration in DMSO (due to solubility limitations of the chromophore in aqueous media).^{21–24} This corresponds to a quenching efficiency E exceeding 95%, calculated according to $E = 1 - (\tau/\tau_0)$, where τ and τ_0 denote the fluorescence lifetimes of the chromophore covalently bound to DNA (τ) and the chromophore without DNA (τ_0), respectively.

The estimated quenching rate constant of $k = 0.16 \times 10^9 \text{ s}^{-1}$ lies within the typical range reported for ultrafast photoinduced electron processes.^{23,25,26} A qualitative Rehm–Weller estimation²³ based on the redox potentials, $\Delta G_{\text{ET}} = E_{\text{ox}} - E_{\text{red}} - E_{00}$ (neglecting the Coulomb interaction E_{C}) of the chromophores supports the thermodynamic feasibility of a photoinduced charge separation in this bichromophore DNA: this charge separation reduces the porphyrin by one electron and oxidizes pyrene, based on the reduction potential of tetraphenylporphyrin $E_{\text{red}} = -1.05$ V (vs. SCE),²⁷ $E_{00} = 3.25$ V^{28,29} and the oxidation potential $E_{\text{ox}} = 1.28$ V (vs. SCE) of pyrene^{28,29} yielding a strongly exergonic driving force $\Delta G_{\text{ET}} = -0.92$ V.²⁹

In conclusion, we have developed a novel, stepwise orthogonal click² strategy performed directly on a solid support after automated DNA synthesis. This approach leverages readily accessible phosphoramidite precursors (EdU and IdU) to incorporate potentially any chromophore modified with an azide or ethynyl function. We representatively tested this synthetic method with a porphyrin and a pyrene that labelled the DNA efficiently. The spectroscopic data indicate that the DNA helix acts as a pre-organized scaffold that positions donor and acceptor chromophores at a distance of approximately 1–1.5 nm, thereby promoting ultrafast electron transfer processes. The almost complete fluorescence quenching in the doubly modified DNA cannot be attributed to extensive structural denaturation or exciton delocalization, but rather to a highly efficient, DNA-mediated non-radiative relaxation mechanism. Our method expands the toolbox for synthesizing complex, multi-chromophoric DNA



assemblies suitable for applications in light-harvesting systems and molecular electronics.

Conflicts of interest

There are no conflicts to declare.

Data availability

The data supporting this article have been included as part of the supplementary information (SI). Supplementary information: all experimental data, procedures for syntheses and spectroscopic experiments. See DOI: <https://doi.org/10.1039/d6cc00319b>.

Acknowledgements

Financial support from the Deutsche Forschungsgemeinschaft (DFG) (grant Wa 1386/27-1), the Fonds der chemischen Industrie (FCI) and the Karlsruhe Institute of Technology (KIT) is gratefully acknowledged.

References

- 1 C. W. Tornøe, C. Christensen and M. Meldal, *J. Org. Chem.*, 2002, **67**, 3057–3064.
- 2 V. V. Rostovstev, L. G. Green, V. V. Fokin and K. B. Sharpless, *Angew. Chem., Int. Ed.*, 2002, **41**, 2596–2599.
- 3 C. Beyer and H.-A. Wagenknecht, *Chem. Commun.*, 2010, **46**, 2230–2231.
- 4 K. Krell, D. Harijan, D. Ganz, L. Doll and H.-A. Wagenknecht, *Bioconjugate Chem.*, 2020, **31**, 990–1011.
- 5 A. El-Sagheer and T. Brown, *Chem. Rev.*, 2010, **39**, 1388–1405.
- 6 M. Shelbourne, X. Chen, T. Brown and A. H. El-Sagheer, *Chem. Commun.*, 2011, **47**, 6257–6259.
- 7 O. S. Wolfbeis, *Angew. Chem., Int. Ed.*, 2007, **46**, 2980–2982.
- 8 K. Gutsmedl, D. Fazio and T. Carell, *Chem. – Eur. J.*, 2010, **16**, 6877–6883.
- 9 M. Aigner, M. Hartl, K. Fauster, J. Steger, K. Bister and R. Micura, *ChemBioChem*, 2011, **12**, 47–51.
- 10 M. B. Walunj and S. G. Srivatsan, *Bioconjugate Chem.*, 2020, **31**, 2513–2521.
- 11 T. R. Chan, R. Hilgraf, K. B. Sharpless and V. V. Fokin, *Org. Lett.*, 2004, **6**, 2853–2855.
- 12 H.-A. Wagenknecht, *Angew. Chem., Int. Ed.*, 2003, **42**, 2454–2460.
- 13 N. Amann, T. Fiebig and H.-A. Wagenknecht, *Chem. – Eur. J.*, 2002, **8**, 4877–4883.
- 14 E. Stulz, *Acc. Chem. Res.*, 2017, **50**, 823–831.
- 15 H. S. Lee, J. H. Han and D. W. Cho, *Phys. Chem. Chem. Phys.*, 2017, **19**, 27123–27131.
- 16 J. S. Lindsey, *Acc. Chem. Res.*, 2010, **43**, 300–311.
- 17 W. Saenger, *Principles of nucleic acid structure*, Springer Science & Business Media, 2013.
- 18 M. Şener, J. Strümpfer, J. Hsin, D. Chandler, S. Scheuring, C. N. Hunter and K. Schulten, *ChemPhysChem*, 2011, **12**, 518–531.
- 19 A. Olaya-Castro and G. D. Scholes, *Int. Rev. Phys. Chem.*, 2011, **30**, 49–77.
- 20 S. G. Telfer, T. M. McLean and M. R. Waterland, *Dalton Trans.*, 2011, **40**, 3097–3108.
- 21 D. Inan, R. K. Dubey, W. F. Jager and F. C. Grozema, *J. Phys. Chem. C*, 2019, **123**, 36–47.
- 22 M. L. Perrin, F. Prins and D. Dulić, *Angew. Chem., Int. Ed.*, 2011, **50**, 11223–11226.
- 23 D. Rehm and A. Weller, *Isr. J. Chem.*, 1970, **8**, 259–271.
- 24 M. R. Wasielewski, *Acc. Chem. Res.*, 2009, **42**, 1910–1921.
- 25 M. R. Wasielewski, *Chem. Rev.*, 1992, **92**, 435–461.
- 26 R. A. Marcus, *J. Electroanal. Chem.*, 1997, **438**, 251–259.
- 27 J. R. Diers, C. Kirmaier, M. Taniguchi, J. S. Lindsey, D. F. Bocian and D. Holten, *Phys. Chem. Chem. Phys.*, 2021, **23**, 19130–19140.
- 28 T. L. Netzel, M. Zhao, K. Nafisi, J. Headrick, M. S. Sigman and B. E. Eaton, *J. Am. Chem. Soc.*, 1995, **117**, 9119–9128.
- 29 N. Amann, E. Pandurski, T. Fiebig and H.-A. Wagenknecht, *Angew. Chem., Int. Ed.*, 2002, **41**, 2978–2980.

